

an Eco RI and Hind III cut plasmacytoma DNA that was hybridized to a ³²P-labeled Msp I fragment derived from chromosome 15 and within 100 base pairs of the translocation point (4) show a rearranged band that corresponds to the translocation as well as an unrearranged band. Both of the rearranged Hind III and Eco RI fragments contain the c-myc gene and sequences from both chromosomes 15 and 12. If the translocated c-myc gene is present in the NIH-3T3 cell transformants, then hybridization of Eco RI or Hind III cut DNA with the Msp I fragment or v-myc probes should show the occurrence of a rearranged band in addition to the unrearranged, NIH-3T3 cell, band. This rearranged band would usually be the same size as the plasmacytoma rearranged band but occasionally might differ since the donor DNA is randomly sheared. Figure 2 shows the result of three different primary transformant DNA's cut with Eco RI and Hind III and hybridized to the Msp I fragment probe (the v-myc probe shows the same result). There is no evidence of a rearranged band in either of the three transformants, only a band corresponding to the unrearranged band that is seen in both the BALB/c and NIH-3T3 cell genomes. The conclusion is that there must be another gene, not the translocated c-myc gene, that is altered in murine plasmacytomas and causes transformation of NIH-3T3 cells in transfection experiments. This situation is similar to the leukemia virus-induced chicken bursal lymphomas in that those tumors have a c-myc gene activated by insertion of retroviral sequences but a different cellular oncogene, unrelated to c-myc, is detected in the NIH-3T3 cell transformation assay (11). These findings indicate there are at least two oncogenes that are altered in both murine plasmacytomas and avian bursal lymphomas and are consistent with the current concept of oncogenesis as a multistep process, although their roles in the generation of lymphoid tumors are unknown.

Thus we have demonstrated a specific chromosomal translocation involving an oncogene in transformed cells (12). The accumulated evidence from karyotypic analysis and molecular cloning suggests that translocation of the c-myc gene is a consistent feature of murine plasmacytomas and seems likely to play a role in the genesis of these tumors. Two other types of alterations of the c-myc gene have been discovered in other tumors. In chicken bursal lymphomas, the c-myc gene is altered by insertion of avian

leukosis virus either 5' or 3' to the gene. The result is an increase in the number of c-myc transcripts with respect to that seen in various untransformed cells (13). Amplification of the c-myc gene has been demonstrated in the human promyelocytic leukemia line HL-60 (14). Amplification of the gene also is accompanied by an increase in the number of transcripts. In plasmacytomas, the precise effect of the translocation on the c-myc gene is unknown; however, this rearrangement could potentially alter transcriptional regulatory sequences, promoter sequences, splice sequences, or coding sequences. In fact, Adams *et al.* (5) report data indicating that the translocated c-myc gene synthesizes transcripts that differ in size from those produced by the untranslocated gene. The availability of clones containing the translocated c-myc gene should allow us to examine the nature and concentration of c-myc transcripts from the rearranged chromosome and determine whether other important alterations in the c-myc sequence accompany the translocation.

STEPHEN CREWS

RICHARD BARTH

LEROY HOOD

*Division of Biology,
California Institute of Technology,
Pasadena 91125*

JOHN PREHN

KATHRYN CALAME

*Department of Biological Chemistry,
University of California, Los Angeles,
Medical School, Los Angeles 90025*

References and Notes

1. G. Klein, *Nature (London)* **294**, 313 (1981).
2. P. D'Eustachio, D. Pravatcheva, K. Marcu, F. H. Ruddle, *J. Exp. Med.* **151**, 1545 (1980); T. Meo, J. Johnson, C. V. Beechey, S. J. Andrews, J. Peters, A. G. Searle, *Proc. Natl. Acad. Sci. U.S.A.* **77**, 550 (1980); D. Swan, P. D'Eustachio, L. Leinwand, J. Seidman, D. Keithley, F. H. Ruddle, *ibid.* **76**, 2735 (1979).
3. I. R. Kirsch, J. V. Ravetch, S.-P. Kwan, E. E. Max, R. L. Ney, P. Leder, *Nature (London)* **293**, 585 (1981); L. Harris, R. B. Lang, K. B. Marcu, *Proc. Natl. Acad. Sci. U.S.A.* **79**, 4175 (1982).
4. K. Calame, S. Kim, P. Lalley, R. Hill, M. Davis, L. Hood, *Proc. Natl. Acad. Sci. U.S.A.*, in press.
5. J. Adams, S. Gerondakis, E. Webb, J. Mitchell, O. Bernard, S. Cory, *ibid.*, in press.
6. E. M. Southern, *J. Mol. Biol.* **98**, 503 (1975).
7. C. J. Sherr, L. A. Fedele, M. Oskarsson, J. Maizel, G. Vande Woude, *J. Virol.* **34**, 200 (1980); N. Kitamura, A. Kitamura, K. Toyoshima, Y. Hirayama, M. Yoshida, *Nature (London)* **297**, 205 (1982); A. Srinivasan, E. P. Reddy, S. A. Aaronson, *Proc. Natl. Acad. Sci. U.S.A.* **78**, 2077 (1981); B. Vennström, L. Fanshier, C. Moscovici, J. M. Bishop, *J. Virol.* **36**, 575 (1980); W. J. DeLorbe, P. A. Luciw, H. M. Goodman, H. E. Varmus, J. M. Bishop, *ibid.* **36**, 50 (1980); L. M. Souza *et al.*, *Proc. Natl. Acad. Sci. U.S.A.* **77**, 5177 (1980).
8. B. Vennström, C. Moscovici, H. M. Goodman, J. M. Bishop, *J. Virol.* **39**, 625 (1981).
9. For review see G. M. Cooper, *Science* **217**, 801 (1982).
10. M. A. Lane, A. Sainten, G. M. Cooper, *Cell* **28**, 873 (1982).
11. G. M. Cooper and P. E. Neiman, *Nature (London)* **292**, 857 (1981).
12. G. L. C. Shen-Ong, E. J. Keath, S. P. E. Piccoli, and M. D. Cole (*Cell*, in press) have also shown that c-myc is translocated in murine plasmacytomas.
13. W. S. Hayward, B. G. Neel, S. M. Astrin, *Nature (London)* **290**, 475 (1981); G. S. Payne, J. M. Bishop, H. E. Varmus, *ibid.* **295**, 209 (1982).
14. S. Collins and M. Groudine, *ibid.* **298**, 679 (1982); R. D. Favera, F. Wong-Staal, R. C. Gallo, *ibid.* **299**, 61 (1982).
15. We thank M. Lane and G. Cooper for providing the S107/NIH-3T3 transformed cell lines and S. Aaronson, J. M. Bishop, M. Cline, and D. Slamon for providing cloned oncogenes. Supported by NIH grants (L.H. and K.C.) and by a postdoctoral fellowship from the Anna Fuller Fund (R.B.).

21 October 1982

Variable Ultrasound Echogenicity in Flowing Blood

Abstract. *Real-time ultrasound imaging of large abdominal veins revealed blood-stream echogenicity of variable intensity. This variability is largely due to the entrance and persistence of tributary blood currents that show different echogenicity. Red cell aggregation is probably an important cause of bloodstream echoes and their variable intensity.*

Ultrasound reflective imaging of flowing bloodstreams has revealed low-amplitude echoes (1-3). In real-time scanning, such echoes have been observed to move with the flow. In this report we describe what we believe to be a previously unreported finding: ultrasonic echoes from the bloodstream of large veins show zonal variability in intensity related to inflow from tributaries. By scanning along veins we found that the echogenicity of the blood in a large vein is significantly affected by the number and intensity of echoes from blood entering from tributaries. Thus tributary blood

that is hypoechoic relative to blood in the collecting vein produces a hypoechoic current that moves downstream in the larger vein and may be traced directly to the tributary. Similar flows have been seen in tributary blood hyperechoic with respect to the prevailing echogenicity of the main venous channel.

An ultrasonic scanner (4) was used to scan directly the surfaces of the inferior vena cava and portal veins surgically exposed in eight dogs anesthetized with nitrous oxide and halothane. Figure 1A shows two distinct hypoechoic zones in an ultrasound cross section of the

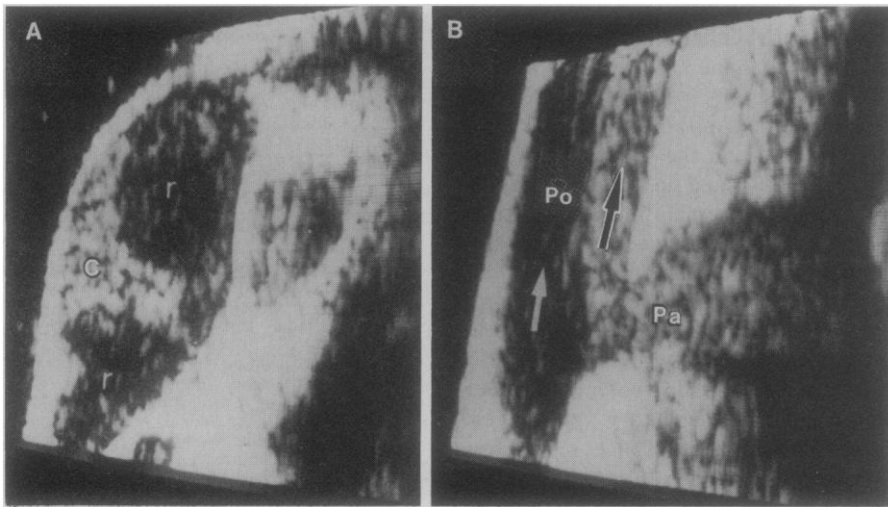


Fig. 1. Sonograms of real-time ultrasound sections of dog vena cava and portal veins. (A) Vena cava in transverse section immediately superior to the entry of the renal veins. The cross section is oval in shape, and three zones of varying echogenicity are distinguishable. Two hypoechoic zones (*r*) are located at the lateral aspects of the caval cross section. A third zone (*c*) of increased echogenicity is between these lateral zones. The hypoechoic zones could be traced directly to the renal veins. (B) Portal vein (*Po*) in longitudinal section at the site of entrance of the pancreatic vein (*Pa*). Echoes in the pancreatic vein are more intense than those in the main portal stream (white arrow) and characterize a current moving toward the liver more slowly (black arrow).

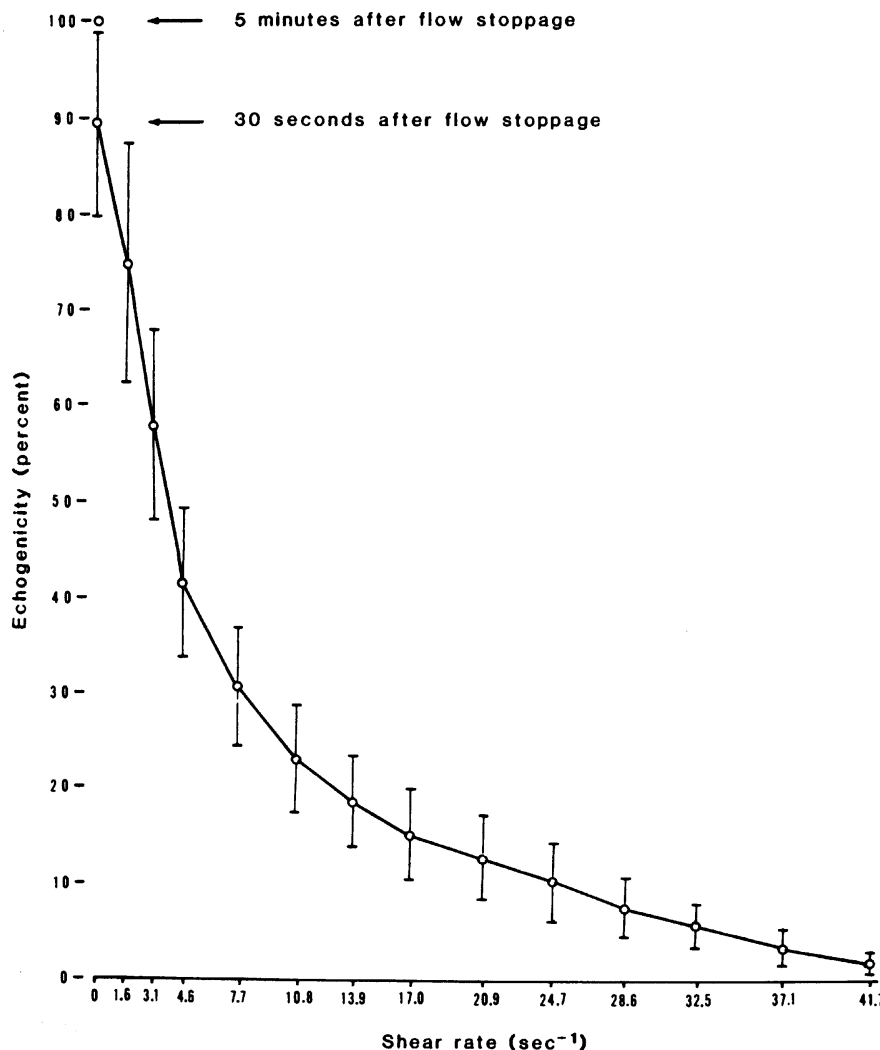


Fig. 2. Relation between echogenicity (expressed as the percentage of maximum echogenicity measured after 5 minutes of complete stasis) and shear rate. Observations were made at progressively lower shear rates and finally at complete stasis. Each point is the mean of 12 measurements. Vertical lines indicate ± 1 standard deviation.

inferior vena cava immediately downstream from the entry of the two renal veins. The renal vein blood showed the same hypoechoic zones in the lateral aspects of the vena cava. Figure 1B shows a longitudinal section through the portal vein at the site where the pancreatic vein enters. Echoes in the pancreatic vein moved toward the portal vein and portal vein echoes moved toward the liver. The pancreatic vein blood was hyperechoic relative to the portal vein blood, and the more echogenic current could be traced downstream in the portal vein for several centimeters.

Explanations offered for the echogenicity of flowing blood point to backscatter from individual red cells, red cell aggregates, and microbubbles (2, 5-7). Although microbubbles and individual red cells reflect ultrasound (for red cells this is particularly true at higher frequencies due to the Rayleigh effect) (8), we believe that red cell aggregation may be a major cause of echogenicity in circulatory systems in which conditions to produce cavitation and microbubbles are absent. At the ultrasound wavelength used in our experiments ($\sim 225 \mu\text{m}$), backscatter from red cell aggregates is more intense than reflected sound from individual red cells. Red cell aggregation has been observed under normal circumstances and is affected by multiple factors such as hematocrit, plasma macromolecules (especially fibrinogen), and shear rate (9). Aggregation is inversely related to shear rate (10) and is regularly observed at shear rates below 46 sec^{-1} .

We previously found that in dogs the echogenicity of blood flowing in the aorta is less intense than that of blood in the vena cava (11). Echogenicity in the vena cava and portal veins increased as flow velocity was decreased by progressive obstruction. These findings could be explained by differences in red cell aggregation produced by different shear rates. We have also found that human blood circulating in tubes is highly echogenic at low shear rates (Fig. 2) (12). At shear rates above 40 sec^{-1} , little echogenicity was noted; as the flow velocity was reduced, echogenicity increased. With each stepwise decrease in flow, echogenicity stabilized at the higher intensity in about 30 seconds. Thus, red cell aggregation and ultrasound echogenicity tend to occur within similar ranges of shear rate. With complete stoppage of flow, maximum echo intensity occurred after 5 minutes. The relatively rapid stabilization of echogenicity at successively decreased flow rates may be explained by the ob-

ervation of Schmid-Schoenbein *et al.* (10) that changes to a new level of shearing quickly established a new dimension for red cell aggregates. Each successive equilibration of aggregate size and number could explain the rapidly occurring stability of echo intensity. With complete stoppage of blood flow (zero shear), red cell aggregation would become maximal. Under these circumstances, red cell aggregates produce a continuous network that is partly suspended by the walls of the blood container (9). This process may require more time than under conditions of blood flow, thus explaining the longer interval needed to produce maximum echogenicity following the onset of stasis.

In previous experiments with static liquid blood, we found that echogenicity of blood is a thixotropic phenomenon that disappears with mechanical agitation and develops seconds after the onset of stasis (13). We also demonstrated that the echogenicity of static blood is directly related to temperature and the concentrations of red cells and macromolecules (such as fibrinogen and gelatin) (14). Finally, we found that peripheral blood from myeloma patients—blood showing increased numbers of rouleaux in smears—is more intensely echogenic than normal blood (14). We conclude that red cell aggregation is an important cause of ultrasound echogenicity in both static liquid blood and flowing blood.

Red cell aggregation may thus explain the observed differences in ultrasound echogenicity in different vessels and in the same vessels. The variable echogenic zones in the inferior vena cava and portal vein may be due to differences in red cell aggregation. Factors such as hematocrit, plasma macromolecules, and shear rate may create differences in red cell aggregation in tributary veins that in turn produce the echogenic variability.

Blood echogenicity could be used as the basis for observing mixing of tributary blood in veins and for noninvasively determining red cell aggregation in vivo in blood vessels opaque to light. Present optical methods of observing aggregation are applicable only to microcirculation. Further study of the relation of echogenicity to red cell aggregation could result in the use of echogenicity or other properties of ultrasonography (such as attenuation of the transmitted sound beam) as a more quantitative measure of aggregation. Finally, these findings may have clinical applications. By controlling the degree of red cell aggregation (as by adjusting the concentration of macromolecules in the circulation), ultrasonic images of blood vessels and perfused

organs may be enhanced. Blood could thus act as a "contrast medium" during ultrasound imaging in medical diagnosis.

BERNARD SIGEL

JUNJI MACHI

JULIO C. BEITLER

JEFFERY R. JUSTIN

JULIO C. U. COELHO

Department of Surgery, University of Illinois College of Medicine, Post Office Box 6998, Chicago 60680

References and Notes

1. R. Gramiak and P. M. Shah, *Radiology* **100**, 415 (1971).
2. M. K. Wolverson *et al.*, *ibid* **140**, 443 (1981).
3. F. Morin and F. Winsberg, *J. Clin. Ultrasound* **10**, 21 (1982).
4. The instrument used was a 7.5-MHz, real-time, B-mode scanner (High Stoy Technological Corp.). The transducer of this instrument was housed in a scan head with a Mylar window for the sound beam and was mechanically driven at 30 sweeps per second through a sector angle of 18°. The transducer was 6 mm in diameter and focused at a distance of 2 cm. Composite resolution of the system was less than 1 mm and tissue penetration was about 6 cm. The scan head was acoustically coupled to the tissue with saline and was kept 1 to 1.5 cm from the surface of the blood vessels. This placed the transducer focal distance approximately in the middle of the lumen of the scanned vessels. The gain of the scanner was set to the highest sensitivity that would permit clear image reception. Further increases in gain markedly distorted the image due to high noise levels.
5. K. P. K. Shung, R. A. Singleman, J. M. Reid, *IEEE Trans. Biomed. Eng.* **23**, 460 (1976).

6. A. Kort and I. Kronzon, *J. Clin. Ultrasound* **10**, 117 (1982).
7. R. S. Meltzer *et al.*, *ibid.*, p. 240.
8. E. U. Condon, *Handbook of Physics* (McGraw-Hill, New York, ed. 2, 1967), pp. 6-112-6-130.
9. S. E. Charm and G. S. Kurlane, *Blood Flow and Microcirculation* (Wiley, New York, ed. 1, 1974), pp. 22-63.
10. H. Schmid-Schoenbein, P. Gaehtgens, H. Hirsch, *J. Clin. Invest.* **47**, 1447 (1968).
11. J. Machi, B. Sigel, J. C. Beitler, J. C. U. Coelho, J. R. Justin, *J. Clin. Ultrasound*, in press.
12. Fresh heparinized blood from 12 normal subjects was circulated through polyvinyl tubing at various velocities by a peristaltic pump. A segment of thin latex tubing 8.8 mm in diameter was interposed in the plastic loop of tubing. Ultrasound imaging with a 10-MHz real-time system was performed on blood flowing through the latex segment. Blood was circulated at progressively lower velocities and echogenicity was measured 30 seconds after onset of a new flow velocity. Shear rate was a relative approximation because it was an estimate of mean shear rate based on the assumption of Newtonian flow and was calculated from the tube radius and average velocity. Mean flow velocity (V) equals $\Delta PR^2/8\eta l$ and mean shear rate (D) equals $\Delta PR/3\eta$, where ΔP is pressure difference over tube length (l), R is tube radius, and η is coefficient of viscosity; by substitution, $D_i = 8V_i/3R_i$ [R. L. Whitmore, Ed., *Rheology of the Circulation* (Pergamon, Oxford, ed. 1, 1968), p. 42]. Echogenicity was determined by measuring the amplitude of ultrasound A-mode reflection at the center of the tubing. Echogenicity of static blood (zero shear) was measured 30 seconds and 5 minutes after flow was stopped. Echogenicity reached its maximum level by 5 minutes. This level of echogenicity was considered 100 percent of measured echogenicity and was used as the reference on the ordinate in Fig. 2.
13. B. Sigel *et al.*, *Invest. Radiol.* **16**, 71 (1981).
14. B. Sigel *et al.*, *ibid.* **17**, 29 (1982).

19 July 1982

Yeast Mating Pheromone Activates Mammalian Gonadotrophs: Evolutionary Conservation of a Reproductive Hormone?

Abstract. α -Factor, a tridecapeptide mating pheromone of yeast (*Saccharomyces cerevisiae*), has extensive sequence homology with the hypothalamic decapeptide gonadotropin-releasing hormone (GnRH). Both synthetic and natural preparations of α -mating factor were found to bind specifically to rat pituitary GnRH receptors and to stimulate the release of luteinizing hormone from cultured gonadotrophs. The ability of the yeast pheromone to reproduce the biological actions of GnRH in the mammalian pituitary gland indicates that the structural and functional properties of GnRH-related peptides may have been highly conserved during evolution.

Unicellular organisms and invertebrates produce a variety of molecules with structural or conformational similarities to the vertebrate hormones and neurotransmitters (1, 2). These include a yeast pheromone that resembles the central regulatory hormone for mammalian reproduction, the hypothalamic neuropeptide known as gonadotropin-releasing hormone (GnRH) or gonadoliberin. This decapeptide is secreted into the pituitary portal system for transport to the adenohypophysis (3), where it binds to plasma-membrane receptors on the gonadotrophs (4) and activates the calcium-dependent release (5) of glycoprotein hormones [luteinizing hormone (LH) and follicle-stimulating hormone (FSH)] which control the endocrine and reproductive functions of the testis and ovary.

Immunoreactive GnRH is also present in the brain (6), placenta (7), and possibly the gonads (8) and milk (9) of mammals. Recently, extrapituitary receptors and actions of GnRH have been described in the rat ovary and testis (10) and in the human placenta (11).

In terms of phylogenetic distribution, mammalian GnRH-like peptides have been described in the hypothalamus and other regions of the nervous system of birds, reptiles, amphibia, and fish. Some of these peptides exhibit minor differences in their amino acid sequence from mammalian GnRH and behave as weak agonists for LH release in cultured rat pituitary cells (6, 12). In bullfrog sympathetic ganglia, the target neurons for an endogenous GnRH-like peptide recognize mammalian GnRH and its potent